Raman scattering of hydrogen storage material $LiNH_2$

Akitaka Michigoe,[1,*] Takumi Hasegawa,[1] Norio Ogita,[1] Masayuki Udagawa,[1,2]
Masami Tsubota,[2] Takayuki Ichikawa,[2] Yoshitugu Kojima,[2] and Shigehito Isobe[3]

[1] *Graduate School of Integrated Arts & Sciences, Hiroshima University, Higashi-Hirosima,739-8521, Japan*
[2] *Institute for Advanced Material Research, Hiroshima University, Higashi-Hiroshima,739-8530, Japan*
[3] *Graduate School of Engineering, Hokkaido University, Sapporo,060-8628, Japan*

(Received April 10, 2010)

Phonon Raman spectra of single crystalline $LiNH_2$ have been measured in the temperature range between 3.5 K and 300 K. The observed peaks are well assigned by the polarization dependence of the single crystal, comparing with the first principles calculation. Below 100K five new peaks appear, and it is concluded that these are caused by the freezing of the rotational motion of NH_2 molecule. It is found that the vibration energy of the Li motion decreases with decreasing temperature. This result shows that the vibration of Li is highly anharmonic with the large amplitude.

PACS numbers: 63.20.-e, 63.20.Ry, 78.30.Hv

I. INTRODUCTION

$LiNH_2$ is known as one of the typical materials in the hydrogen storage material, especially for the application to motor vehicle. Its advantage is lightweight and reusable, but at this stage it needs the high reaction temperature above 473 K (200 °C). Thus, lower reaction temperature and fast kinetics are required in the reactions. $LiNH_2$ releases H_2 around 473 K–673 K in the following successive reactions by the sake of LiH and NH_3 [1, 2].

$$2LiNH_2 \longrightarrow Li_2NH + NH_3 \qquad \text{and} \qquad LiH + NH_3 \longrightarrow LiNH_2 + H_2.$$

The entire reaction is reversible and is given by

$$LiNH_2 + LiH \longleftrightarrow Li_2NH + H_2.$$

At this stage, the mechanism of the reactions at the atomic level is not well understood. Raman scattering is very useful to obtain the information of the atomic level. In the reported Raman scattering experiments, the employed samples were polycrystalline, where the precise assignment of the observed peaks is very difficult due to lack of the precise polarization dependence, especially for the low energy phonon peaks [3–7]. Thus, in this study we have employed the single crystalline $LiNH_2$ and have tried to assign the observed peaks at room temperature by the polarization dependence, comparing with the results of

the first principles calculation. In addition, we have measured the Raman scattering spectra in the temperature region between 3.4 K and 300 K to clarify the dynamical property of Li and NH_2 molecules.

II. EXPERIMENT

The employed single crystal $LiNH_2$ was grown by a Tamman method from liquid $LiNH_2$. The crystal was kept in argon atmosphere to avoid oxidation and water adsorption.

Raman scattering spectra were measured by a triple-monochromator (JASCO, model NR-1800) with a liquid N_2 cooled CCD detector (Princeton Instruments, model LN/CCD-1100-PB). An Ar^+ laser was used as the excitation light. The wavelength of the excitation light was 514.5 nm and the light was linearly polarized. At room temperature, we measured Raman spectra of $LiNH_2$ using microscope system. For the low temperature measurement from 3.4 K to 300 K, the macro Raman scattering system was employed. Power of laser light was 2.5 mW at the specimen in the case of the microscope system and 15 mW for the macro measurement.

Crystal structure of $LiNH_2$ is tetragonal, and space group is I-4 [8]. In this symmetry and structure, group theory gives us 7A + 8B + 9E for phonons and 3A + 3B + 3E for the molecular vibrations of NH_2. Here, A, B and E are irreducible representations. They are all Raman active phonons and E modes are doubly degenerate. Thus 33 peaks will appear in the Raman spectra.

The phonons with each irreducible representation can be determined by the polarization dependence. The polarization geometry is given by a symbol of (i,s), where i and s denote the polarization directions of incident and scattered light, respectively. The modes with each irreducible representation appear in the following geometries: (x,x), (y,y), or (z,z) for A, (x,y) or (x+y,x−y) for B, and (x,z) or (y,z) for E. In the ordinary case the principle axes of the unit cell are employed for x, y, and z, that is, x corresponds to [1,0,0], y to [0,1,0], and z to [0,0,1]. Thus, if the normal direction of the crystal surface is parallel to one principle axis, the assignment of the observed peak can be made by one spectrum. Unfortunately in the present case, the [0,0,1] direction inclines from the normal direction of the sample surface. In this case the additional experiments due to the detailed angle dependence are necessary. The method and results are presented in the next section.

III. RESULTS AND DISCUSSION

Raman scattering intensity I is given by

$$I = \left(\sum_{\alpha\beta} E^i_\alpha R_{\alpha\beta} E^s_\beta \right)^2 , \tag{1}$$

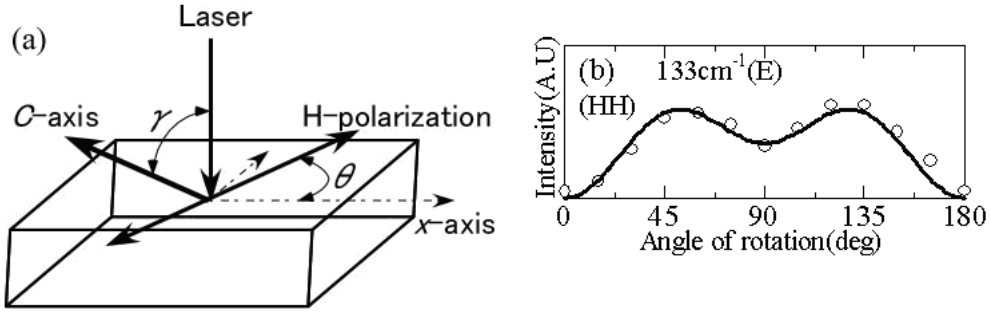

FIG. 1: (a) Sample geometry. H is the polarization direction of laser beam. γ is the angle between the normal direction of the surface and the c-axis. θ is the rotation angle of the H direction. In the experiment, we rotated the sample. (b) Open circles denote the observed intensity of the E-symmetry mode at 133 cm^{-1} in (HH). Bold line is the calculated intensity of the E mode as a function of θ for $\gamma = 64°$.

where R is Raman tensor; E^i and E^s are electric field of incident and scattered light, respectively. Suffix α and β are Cartesian coordinate. As shown in Fig. 1(a), the c-axis of our sample inclines from the normal axis of the sample surface with the angle of γ. The polarization direction of the incident and scattered light are on the horizontal plane. We employed two polarization geometries denoted by (HH) and (HV). θ is the angle between x and H directions. We have measured the angle dependence of θ in the 15° step for both (HH) and (HV). The angle dependence of the scattered intensity in the (H,H) geometry for the E symmetry is given as

$$I_{E,HH} = C_{ehh}\left(\sin^2\gamma\sin^2 2\theta + \sin^2 2\gamma\sin^4\theta\right), \tag{2}$$

where the coefficient C_{ehh} is related with the values of Raman tensor components. The intensity is determined by the angle γ. Thus, we can experimentally determine the angle γ. The best fitted curve for the E-symmetry mode at 133 cm^{-1} is shown in Fig. 1(b), where $\gamma = 64°$. For the A symmetry mode, the (H,V) geometry shows the similar θ dependence as given by eq. (3),

$$I_{A,HV} = C_{ahv}\sin^2 2\theta \tag{3}$$

where C_{ahv} also does not depends on the modes. However, for the B-symmetry mode, the coefficient depends on the mode. Therefore, in addition to the θ dependence of the scattered intensity at $\gamma = 64°$, we have assigned A and B modes, referring with the first principle calculation results.

The representative Raman scattering spectra, measured at room temperature, are shown in Fig. 2, where $\theta = 45°$ step spectra are presented for both (H,H) and (H,V) geometries. As the results, we can divide three energy regions: Lattice vibrations due to Li and NH_2 molecules below 700 cm^{-1} (Phonon region), NH_2 bending modes in the energy region between 1500 and 1600 cm^{-1}, and NH_2 stretching vibrations from 3200 to 3400

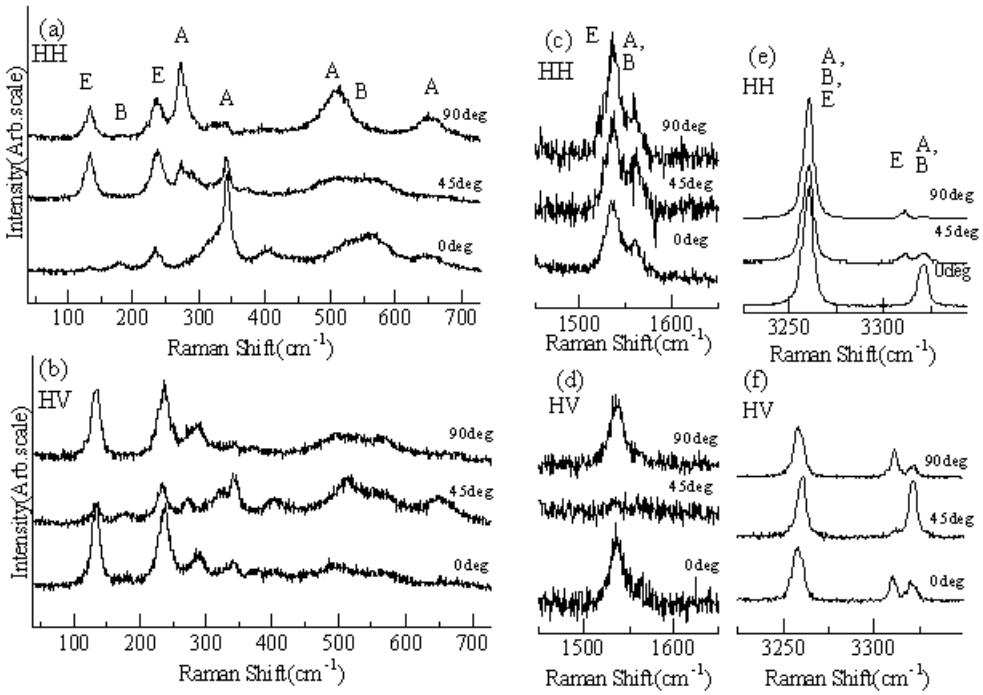

FIG. 2: Raman spectra measured at room temperature. Rotation angle with $\theta = 45°$ step are presented. (a) and (b) show the phonon region spectra in the (HH) and (HV) geometries, respectively, (c) and (d) bending mode spectra, and (e) and (f) stretching mode spectra.

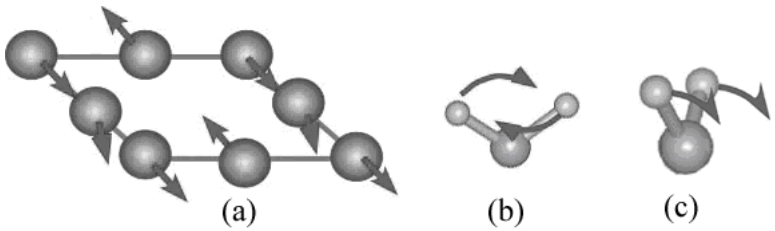

FIG. 3: Atom displacements of the representative phonon obtained from first principles calculation. (a): Li atoms vibration with the E-symmetry at 133 cm^{-1}. (b): Twisting mode of NH_2 at 513 cm^{-1}. (c): Wagging mode of NH_2 at 654 cm^{-1}.

cm^{-1}. In the figure, the assigned symmetry of the observed peaks is also shown, using the results of the polarization dependence.

The assignment of the observed modes at room temperature (Obs.) is summarized in Table I, where the modes numbered No.1–24 corresponds to the phonon mode region, 25–27 to the bending modes of NH_2, and 28–33 to the stretching mode of NH_2. The results of the first principle calculation are also listed in the fourth column (Cal.).

TABLE I: Assignment of the observed peaks in $LiNH_2$ at room temperature.

No	Sym.	Obs.	Cal.	No	Sym.	Obs.	Cal.	No	Sym.	Obs.	Cal.
1	E	133	109	12	B		338	23	E		679
2	B	178	184	13	A	343	348	24	B		719
3	E		195	14	E		385	25	E	1536	1435
4	A		210	15	A		404	26	B	1560	1485
5	E	238	239	16	B	406	419	27	A	1560	1502
6	B		257	17	B		457	28	A	3260	3257
7	A	272	275	18	E		500	29	E	3260	3263
8	E	289	279	19	A	513	515	30	B	3260	3265
9	A		305	20	E		569	31	E	3310	3345
10	B		312	21	B	563	600	32	B	3321	3346
11	E	322	317	22	A	655	669	33	A	3321	3348

Figure 3 shows the atom displacements of the representative modes in the phonon region. They are derived from the first principles calculation. We note that the lowest energy mode is the Li vibration and the modes due to NH_2 rotation appear at 400–700cm^{-1}.

Figure 4 shows the temperature dependence of the representative phonon region spectra below room temperature. All peaks become sharp with decreasing temperature. Below 100 K, new peaks appear and are depicted by open triangles in the figure. These new peaks appear as the satellite peak of the main peaks, except for the peak at 450 cm^{-1}. The main peak symmetry is not only E, but also A and B. If the main peak symmetry is only E-symmetry, origin might be the broken of the degeneracy between a- and b-axes in the tetragonal structure. This leads to the structural transition. However, since the A- and B-symmetries are one dimensional representation, we cannot explain the origin of the new peaks by the structural change. Therefore, the possible origin of the new peaks is the

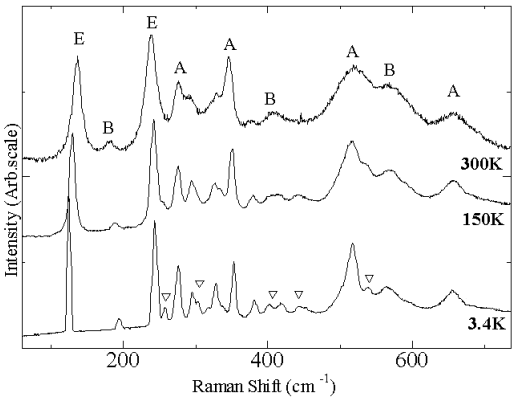

FIG. 4: Temperature dependence of phonon Raman spectra. New peaks depicted by triangles clearly appear at low temperature.

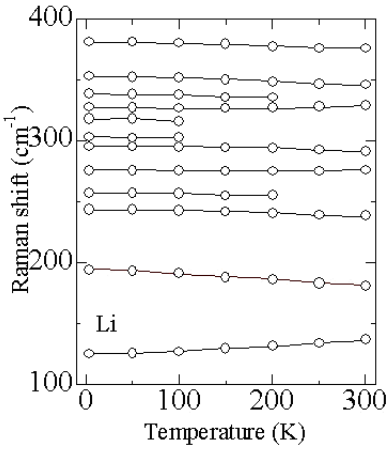

FIG. 5: Temperature dependence of the phonon energies. It should be noted that the energy of Li vibration decreases with decreasing temperature.

change of the dynamical property of NH_2, that is, the freezing of the rotational motion of NH_2 below 100K. In order to confirm this conclusion, NQR experiment of NH_2 is necessary and remains as the future task.

Figure 5 shows the temperature dependence of the vibration energy of the phonon region modes. Except for the lowest energy mode due to Li motion, all energies increase with decreasing temperature. This temperature dependence is an ordinary case, since the energy increase is understood by the thermal shrinkage effect of volume. However, as shown in the figure, the vibration energy of the Li mode shows the different temperature dependence. The energy decreases with decreasing temperature. This phenomenon has been observed in the caged compounds (type-I clathrates [9–11], KOs_2O_6 [11, 12], filled skutterudites [13, 14], and $La_3Pd_{20}Ge_6$ [11, 15]) and layered compound of CaAlSi [16]. This temperature dependence has been already understood by the fourth order anharmonic effect. Thus, the Li vibration is highly anharmonic with large amplitude [9].

At low temperatures, the peak width of the bending and stretching modes of NH_2 becomes sharp and no anomalous change of the spectral shape has been observed. However, it is found that the energy of NH_2 bending (scissors) vibration decreases with decreasing temperature. This will be understood by the decrease of the bond angle at low temperature. On the other hand, the energy increase of NH_2 stretching vibrations indicates that bond length becomes shorter at low temperature.

IV. CONCLUSIONS

We have measured Raman spectra of single crystalline $LiNH_2$. The observed peaks are well assigned by the polarization measurement by the sake of the first principles calculation at room temperature. New peaks have been observed below 100 K in the phonon re-

gion. The symmetry consideration concludes that the rotational vibration of NH_2 molecules freezes below 100 K. With decreasing temperature, the energy decrease of the Li mode shows that the Li vibration is highly anharmonic with the large amplitude.

Acknowledgments

This work is partially supported by the Grants of the NEDO project "Advanced Funda-mental Research on Hydrogen Storage Materials". This work is also supported by Grant-in-Aids for Scientific Research on Innovative Areas "Heavy Electrons" (No. 20102005) of The Ministry of Education, Culture, Sports, Science, and Technology, Japan, and supported by N-BARD and IAMR of Hiroshima University.

References

* Electronic address: akitaka-michigoe@hiroshima-u.ac.jp

[1] T. Ichikawa, S. Isobe, N. Hanada, and H. Fujii, J. Alloys and Comp. **365**, 271 (2004).
[2] S. Hino, T. Ichikawa, N. Ogita, M. Udagawa, and H. Fujii, Chem. Commun. **24**, 3038 (2005).
[3] J.-P. O. Bohger, R. R. Essmann, and H. Jacobs, J. Mol. Struct. **348**, 325 (1995).
[4] R. S. Chellap, D. Chandra, M. Somayazulu, S. A. Gramsh, and R. J. Hemley, J. Phys. Chem. **111**, 10785 (2007).
[5] Y. Nakamori and S. Orimo, J. Alloys Comp. **370**, 271 (2004).
[6] Y. Nakamori, T. Yamagishi, M. Yokoyama, and S. Orimo, J. Alloys Comp. **377**, L1(2004).
[7] Y. Nakamori and S. Orimo, Mat. Sci. and Eng. B **108**, 48 (2004).
[8] M. H. Sorby, Y. Nakamura, H. W. Brink, T. Ichikawa, S. Hino, H. Fujii, and B. C. Hauback, J. Alloys Comp. **428**, 297 (2007).
[9] Y. Takasu, T. Hasegawa, N. Ogita, M. Udagawa, M. A. Avila, K. Suekuni, I. Ishii, T. Suzuki, and T. Takabatake, Phys. Rev. B **74**, 174303 (2006).
[10] Y. Takasu, T. Hasegawa, N. Ogita, M. Udagawa, M. A. Avila, K. Suekuni, and T. Takabatake, PRL **100**, 165503 (2008).
[11] M. Udagawa, T. Hasegawa, Y. Takasu, N. Ogita, K. Suekuni, M. A. Avila, T. Takabatake, Y. Ishi-kawa, N. Takeda, Y. Nemoto, T. Goto, H. Sugawara, D. Kikuchi, H. Sato, C. Sekine, I. Shirotani, J. Yamaura, Y. Nagao, and Z. Hiroi, J. Phys. Soc. Jpn. **77** Suppl. A, 142 (2008).
[12] T. Hasegawa, Y. Takasu, N. Ogita, M. Udagawa, J. Yamaura, Y. Nagao, and Z. Hiroi, Phys. Rev. B **77**, 064303 (2008).
[13] K. Iwasa, M. Kohgi, H. Sugawara, and H. Sato, Physica B **378**–**380**, 194 (2006).
[14] S. Tsutsui, H. Kobayashi, J. P. Sutter, H. Uchiyama, A. Q. R. Baron, Y. Yoda, D. Kikuchi, H. Suga-wara, C. Sekine, I. Shirotani, A. Ochiai, and H. Sato, J. Phys. Soc. Jpn. **77** Suppl. A, 257 (2008).
[15] T. Hasegawa, Y. Takasu, T. Kondou, N. Ogita, M. Udagawa, T. Yamaguchi, T. Watanabe, Y. Nemoto, and T. Goto, J. Mag. Mag. Mat. **310**, 984 (2007).
[16] S. Kuroiwa, T. Hasegawa, T. Kondo, N. Ogita, M. Udagawa, and J. Akimitsu, Phys. Rev. B **78**, 184303 (2008).